

## Thermal phase transition in nuclear multifragmentation: The role of Coulomb energy and finite size

B. K. Srivastava,<sup>1</sup> S. Albergo,<sup>2</sup> F. Bieser,<sup>6</sup> F. P. Brady,<sup>3</sup> Z. Caccia,<sup>2</sup> D. A. Cebra,<sup>3</sup> A. D. Chacon,<sup>7</sup> J. L. Chance,<sup>3</sup> Y. Choi,<sup>1</sup> S. Costa,<sup>2</sup> J. B. Elliott,<sup>1</sup> M. L. Gilkes,<sup>1</sup> J. A. Hauger,<sup>1</sup> A. S. Hirsch,<sup>1</sup> E. L. Hjort,<sup>1</sup> A. Insolia,<sup>2</sup> M. Justice,<sup>5</sup> D. Keane,<sup>5</sup> J. C. Kintner,<sup>3</sup> V. Lindenstruth,<sup>4</sup> M. A. Lisa,<sup>6</sup> H. S. Matis,<sup>6</sup> M. McMahan,<sup>6</sup> C. McParland,<sup>6</sup> W. F. J. Müller,<sup>4</sup> D. L. Olson,<sup>6</sup> M. D. Partlan,<sup>3</sup> N. T. Porile,<sup>1</sup> R. Potenza,<sup>2</sup> G. Rai,<sup>6</sup> J. Rasmussen,<sup>6</sup> H. G. Ritter,<sup>6</sup> J. Romanski,<sup>2</sup> J. L. Romero,<sup>3</sup> G. V. Russo,<sup>2</sup> H. Sann,<sup>4</sup> R. P. Scharenberg,<sup>1</sup> A. Scott,<sup>5</sup> Y. Shao,<sup>5</sup> T. J. M. Symons,<sup>5</sup> M. Tincknell,<sup>1</sup> C. Tuvé,<sup>2</sup> S. Wang,<sup>5</sup> P. Warren,<sup>1</sup> H. H. Wieman,<sup>6</sup> T. Wienold,<sup>6</sup> and K. Wolf<sup>7</sup>

(EOS Collaboration)

<sup>1</sup>Purdue University, West Lafayette, Indiana 47907

<sup>2</sup>Università di Catania and Istituto Nazionale di Fisica Nucleare-Sezione di Catania, I-95129 Catania, Italy

<sup>3</sup>University of California, Davis, California 95616

<sup>4</sup>GSI, D-64220 Darmstadt, Germany

<sup>5</sup>Kent State University, Kent, Ohio 44242

<sup>6</sup>Nuclear Science Division, Lawrence Berkeley National Laboratory, Berkeley, California 94720

<sup>7</sup>Texas A&M University, College Station, Texas 77843

(Received 5 September 2000; published 19 September 2001)

A systematic analysis of the moments of the fragment size distribution has been carried out for the multifragmentation of 1A GeV Au, La, and Kr on carbon. The breakup of Au and La is consistent with a continuous thermal phase transition. The data indicate that the excitation energy per nucleon and isotopic temperature at the critical point decrease with increasing system size. This trend is attributed primarily to the increasing Coulomb energy with finite size effects playing a smaller role.

DOI: 10.1103/PhysRevC.64.041605

PACS number(s): 25.70.Pq, 05.70.Jk, 21.10.Sf

The EOS collaboration has recently studied the multifragmentation (MF) of 1A GeV Au on carbon [1–10]. One of the important results was the possible observation of critical behavior and the extraction of associated critical exponents [1,3,5]. The values of these exponents were very close to those of ordinary fluids indicating that MF may arise from a continuous phase transition and may belong to the same universality class as ordinary fluids. Another important result was the successful description of the EOS MF data by statistical thermodynamical models, which describe quantum mechanically the MF of a charged nucleus [10–15]. In this paper we analyze the recent results for MF of 1A GeV La and Kr on C [8] along with those previously reported for Au [1,3,5] in the manner proposed by Campi [16–18]. Our analysis provides the first experimental evidence for the evolution of the MF mechanism with increasing projectile size and for the effects of Coulomb energy and finite size.

The reverse kinematics experiments and the analysis by which the equilibrated remnant, which undergoes MF, was separated from promptly emitted particles as well as the details of the determination of the remnant mass and excitation energy are given in our earlier publications [2,4,8].

Campi [16–18] and Bauer *et al.* [19,20] first suggested that the methods used in percolation studies may be applied to MF data. In percolation theory the moments of the cluster distribution contain the signature of critical behavior [21]. The method of moments analysis was used by several groups [22–25] to search for evidence of the liquid-gas phase transition in MF. Thus for each event, we determine the total multiplicity of charged fragments,  $m$ , and the number of charged fragments  $n_A$ , of nuclear charge  $Z$  and mass  $A$  [2].

We calculate the  $k$  moments of the cluster size distribution given by

$$M_k(m) = \sum A^k n_A(m), \quad (1)$$

where the sum runs over all masses in the event including neutrons except for the heaviest fragment. This quantity was instrumental in extracting the critical exponents in Au+C data [1]. It has been argued that there should be an enhancement in the critical region of the moments,  $M_k$ , for  $k > \tau - 1$ , with critical exponent  $\tau > 2$  [16,17]. For example, the reduced variance  $\gamma_2$ , i.e., the combination of moments given by

$$\gamma_2 = M_2 M_0 / M_1^2 \quad (2)$$

has a peak value of 2 for a pure exponential distribution,  $n_A \sim e^{-\alpha A}$ , regardless of the value of  $\alpha$ , but  $\gamma_2 > 2$  for a power law distribution,  $n_A \sim A^{-\tau}$ , provided the system is large enough. Here  $M_1$  and  $M_2$  are the first and second moments of the mass distribution in an event and  $M_0$  is the total multiplicity including neutrons.

We have calculated  $\gamma_2$  event by event as a function of total charged particle multiplicity for all three systems, as shown in Fig. 1. It is clear that for Au and La,  $\gamma_2 > 2$  at the peak, while for Kr,  $\gamma_2 < 2$ . The position of the maximum  $\gamma_2$  value defines the critical point  $m_c$ , where the fluctuations in the fragment sizes are the largest. To obtain  $m_c$  accurately for each system a high resolution version of Fig. 1, with points corresponding to each value of  $m$ , was fitted with a polynomial of order 3–9 and the fit with the best  $\chi^2$  per degree of

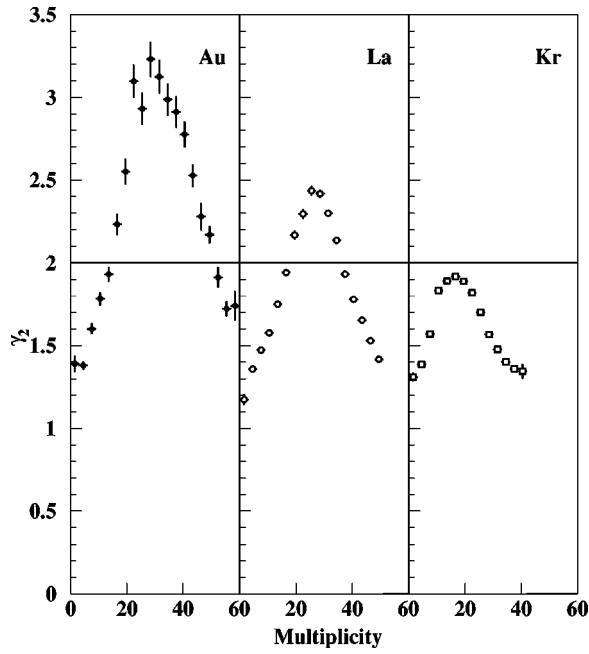


FIG. 1.  $\gamma_2$  as a function of multiplicity from Au, La, and Kr systems.

freedom was then chosen to locate the multiplicity at which  $\gamma_2$  reaches a maximum. The decrease in  $\gamma_2$  with decrease in system size observed in Fig. 1 is also seen in three-dimensional percolation studies and has been attributed to finite size effects [18].

Another way of identifying the critical point is from the fluctuations in the size of the largest fragment. The fluctuations in this quantity,  $\Delta_{A_{\max}}$ , peak at the critical point as shown in Fig. 2(a). For Kr the peak in  $\Delta_{A_{\max}}$  is not as well defined as for Au and La. One sees a peak in  $\Delta_{A_{\max}}$  for Kr at

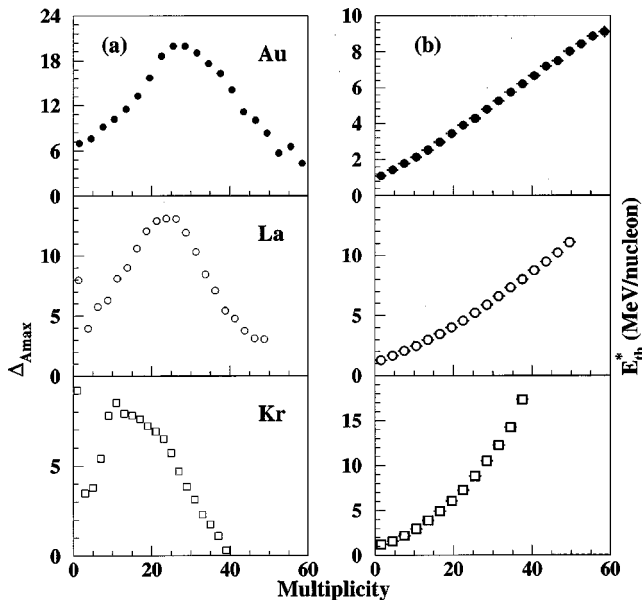


FIG. 2. (a) Fluctuations in the size of the the largest fragment as a function of multiplicity. (b) Excitation energy as a function of multiplicity.

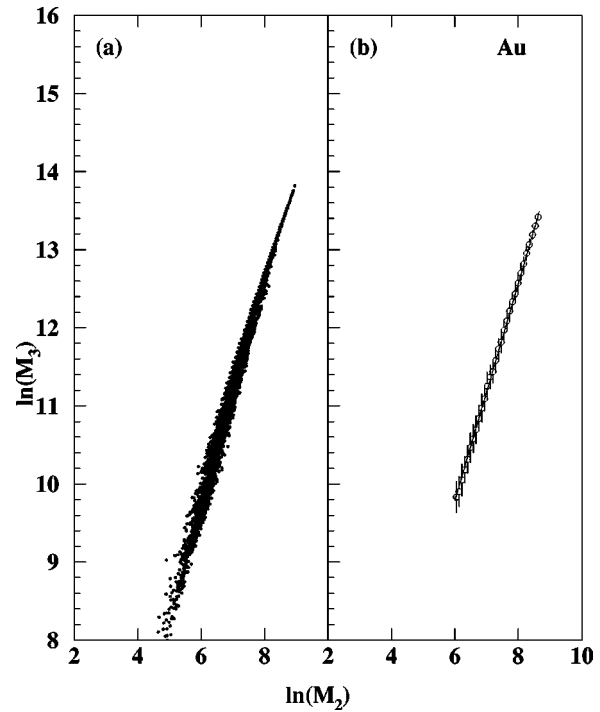


FIG. 3. (a)  $\ln(M_3)$  vs  $\ln(M_2)$  for Au above the critical multiplicity. (b) The average value of  $\ln(M_3)$  at a given  $\ln(M_2)$ .

$m \sim 10$ . This corresponds to  $\sim 3$  MeV/nucleon excitation energy, which is too low for MF to occur. Thus in the case of Kr the  $m_c$  value was obtained from Fig. 1 only. For Au and La,  $m_c$  was obtained as the average of the two peak values in Figs. 1 and 2. The  $m_c$  values for Au, La, and Kr are  $28 \pm 3$ ,  $24 \pm 3$ , and  $18 \pm 2$ , respectively. The  $m_c$  value for Au is in agreement with our earlier reported values for Au within the respective uncertainties [1,5].

The thermal excitation energy,  $E_{th}^*$ , i.e., the energy available for particle and fragment emission, is a more fundamental quantity than the multiplicity. The experimental relation between these two quantities [8] is shown in Fig. 2(b).

To extract the power law exponent  $\tau$ , we examine the MF region above  $m_c$ , i.e., the region past the peak in Fig. 1 [26]. Figure 3(a) shows a scatter plot of  $\ln(M_3)$  vs  $\ln(M_2)$  for Au [1,16,22]. The slope  $S$  of the line through the points is related to the exponent  $\tau$ ,  $S = (\tau - 4)/(\tau - 3)$ . To obtain  $\tau$  we plot the average value of  $\ln(M_3)$  vs  $\ln(M_2)$ , Fig. 3(b). We fit the region between  $E_{th}^* = 5.5 - 7.5$  MeV/nucleon to obtain the  $\tau$  value. The lower energy is  $\sim 1$  MeV/nucleon higher than the energy corresponding to the peak in  $\gamma_2$  and the higher value is close to the end of  $\gamma_2$  branch above  $m_c$  in Fig. 1. We obtain  $\tau = 2.16 \pm 0.08$  for Au with  $\chi^2/\text{DOF}$  of 1. This value is in agreement with the  $\tau$  value from the single parameter fit,  $n_A = q_0 A^{-\tau}$ , at  $m_c$  [5,21]. The same procedure was followed to fit  $\ln(M_3)$  vs  $\ln(M_2)$  for La as shown in Fig. 4(b), derived from the scatter plot for La in Fig. 4(a). For La we obtain  $\tau = 2.10 \pm 0.06$ , with  $\chi^2/\text{DOF} \sim 6$ , again in agreement with the value obtained from the one-parameter fit at  $m_c$ .

The data for Kr are shown in Fig. 5(a). There is a distinct difference between Figs. 3(a), 4(a), and 5(a). In the plot for Au,  $\ln(M_3)$  and  $\ln(M_2)$  lie on a very narrow band while for

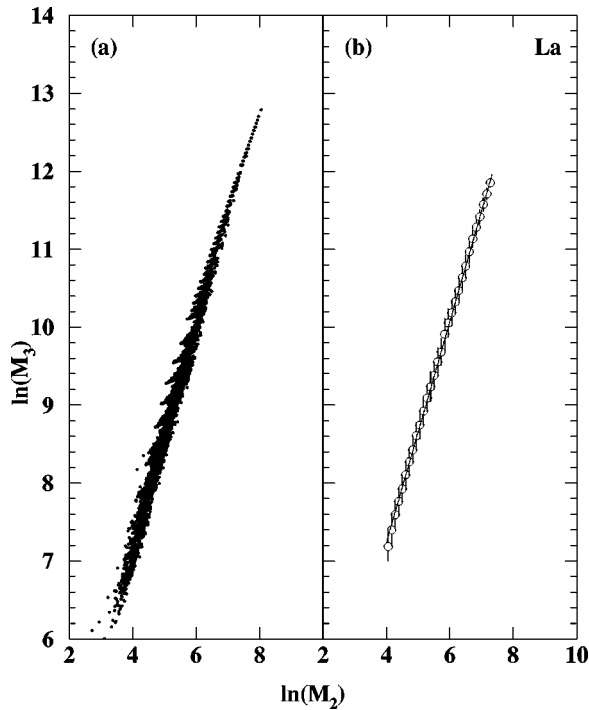


FIG. 4. (a)  $\ln(M_3)$  vs  $\ln(M_2)$  for La above the critical multiplicity. (b) The average value of  $\ln(M_3)$  at a given  $\ln(M_2)$ .

Kr there is a large variation. This difference reflects a wider fragment mass distribution for different events with the same multiplicity for Kr. A similar trend with system size is seen in percolation indicating that this is a finite size effect [26]. Figure 5(b) shows the fit for Kr. A nonlinear behavior is

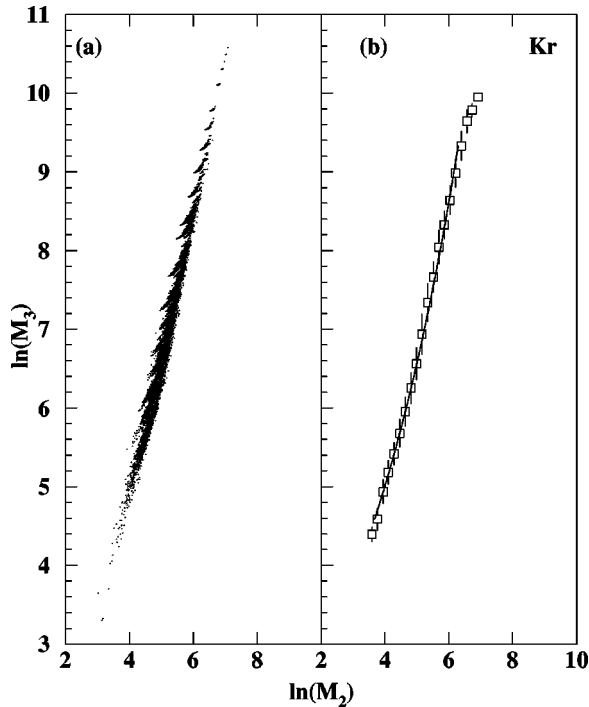


FIG. 5. (a)  $\ln(M_3)$  vs  $\ln(M_2)$  for Kr above the critical multiplicity. (b) Average  $\ln(M_3)$  as a function of  $\ln(M_2)$ .

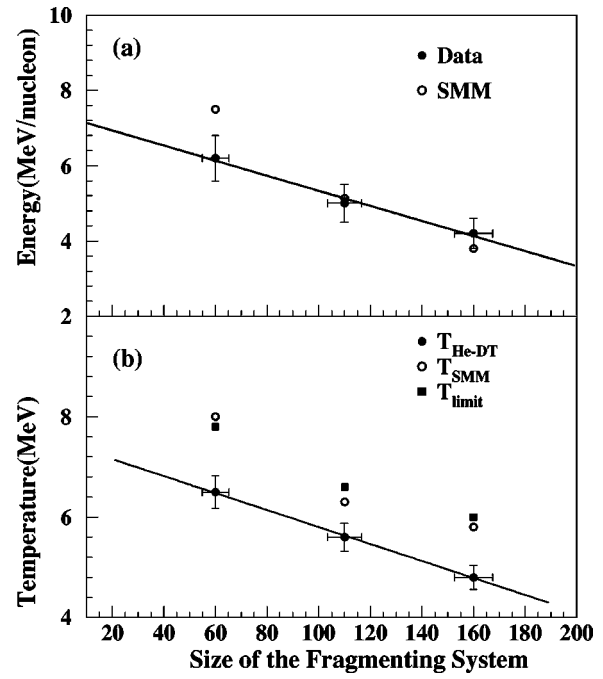


FIG. 6. (a) Energy (MeV/nucleon) at  $m=m_c$ . (b)  $T_{He-DT}$ ,  $T_{SMM}$ , and  $T_{limit}$  as a function of the system size. The lines through the points are linear fits to the data.

clearly observed. This contrasts with the linear behavior seen in the corresponding plots for Au and La in Figs. 3(b) and 4(b), respectively. An exponential fit to the data is shown in Fig. 5(b) to guide the eye. The fitting region was chosen by the criteria laid down in case of Au and La. A linear fit to the Kr data gives a value of  $\tau = 1.88 \pm 0.08$  with an unacceptably large  $\chi^2/\text{DOF}$  of 20. This result is consistent with Fig. 1, in which the peak  $\gamma_2$  value is  $< 2$  for Kr.

The thermal excitation energy per nucleon at  $m_c$ ,  $E_c^*$ , was obtained for each system from the variation of  $E_{th}^*$  with  $m$  as shown in Fig. 2(b). The dependence of  $E_c^*$  on system size is shown in Fig. 6(a), where the size of fragmenting system is the average remnant mass at  $m_c$  [8]. The width of the remnant mass distribution at  $m_c$  is indicated by the horizontal error bars and is  $\sim 6-8\%$  [4,8]. Figure 6(b) shows the isotope freeze-out temperature,  $T_{He-DT}$ , obtained from the  $H^2/H^3$  and  $He^3/He^4$  double isotope ratios at  $m_c$  [8,27]. Both  $E_c^*$  and  $T_{He-DT}$  decrease with increasing system size. We can compare these results with calculations that have studied highly excited nuclear matter. The temperature-dependent Hartree-Fock (HF) calculations for equilibrated hot nuclei show that Coulomb repulsion causes the compound nucleus to become unstable at a lower temperature than the uncharged system [28]. The trend seen in the present work is also seen in a HF calculation using a Skyrme interaction with a soft equation of state [29]. This temperature is shown in Fig. 6(b) as  $T_{limit}$ . In another study [30] it was found that finite size effects and Coulomb force lead to a considerable reduction in the “critical” temperature.

The Au, La, and Kr results can also be compared with the statistical multifragmentation model (SMM) [10,11]. The SMM  $E_c^*$  values are shown in Fig. 6(a). The agreement be-

tween data and SMM is good although a  $\sim 1$  MeV/A discrepancy is observed for Kr. The SMM breakup temperature  $T_{\text{SMM}}$  [11] is shown in Fig. 6(b). There is a decrease in both temperatures with increasing system size. It is apparent that the  $T_{\text{He-DT}}$  temperature is about 1 MeV lower than the SMM temperature. This difference is due to the fact that  $T_{\text{He-DT}}$  is measured after secondary decay has taken place, while  $T_{\text{SMM}}$  corresponds to the breakup configuration. Particularly interesting is the fact that the experimental  $T_{\text{He-DT}}$  tracks  $T_{\text{SMM}}$  in its dependence on system size at  $m_c$ . SMM indicates that the decrease in both  $T_{\text{SMM}}$  and in  $E_c^*$  with increasing system size is due to the increase of the Coulomb energy. This result suggests that the Coulomb energy plays a central role in the MF of nuclei.

The microcanonical Metropolis Monte Carlo [12,13] calculations have emphasized that MF is controlled by the competition between long range Coulomb forces and finite size effects. Finite size effects in models with only short range forces predict an *increase* in the critical temperature as the system size increases, as is evident from percolation [31] and Ising model studies [32]. Since the experimental temperature exhibits the opposite dependence on system size, it is apparent that Coulomb effects are more important than finite size effects. For finite *neutral* matter the critical temperature ( $T_c$ ) is expected to be  $\sim 15$ – $20$  MeV [30,33]. The observed  $T_c$  for  $A = 160$  is  $\sim 6$  MeV. Compared to finite uncharged nuclei, the

presence of Coulomb energy plays a role in lowering the excitation energy needed to reach the regime where critical signatures are observed. In the smaller Kr system there is less Coulomb energy in the initial remnant state. Achieving multifragmentation in this system requires greater excitation energy/nucleon compared to Au and La (as shown in Fig. 6) and as a result, the dynamics of the ensuing disassembly may not take this system near its critical regime.

In conclusion, we have analyzed the fragment distributions resulting from 1A GeV Au, La, and Kr on carbon. The reduced variance  $\gamma_2$  has a peak at the multiplicity where the fluctuations in  $A_{\text{max}}$  are largest. The peak value of  $\gamma_2$  is  $>2$  for Au and La and they exhibit a power law fragment yield distribution at  $m_c$ . The peak value for Kr is  $<2$  and this system does not exhibit a power law with  $\tau \geq 2$ . The decrease in  $\gamma_2$  with decreasing system size can be attributed to finite size effects. These observations argue against a continuous phase transition in the MF of Kr but are consistent with such a transition in the MF of La and Au. Recent analysis based on the SMM microcanonical caloric curve [10], which indicated a first order phase transition for the MF of Kr and a continuous phase transition for the MF of Au is consistent with experimental observations. The observed decrease in excitation energy and temperature with an increase in system size for MF at the critical point shows the importance of the Coulomb energy in MF.

This work was supported by the U.S. Department of Energy.

- 
- [1] M. L. Gilkes *et al.*, Phys. Rev. Lett. **73**, 1590 (1994).
  - [2] J. A. Hauger *et al.*, Phys. Rev. Lett. **77**, 235 (1996).
  - [3] J. B. Elliott *et al.*, Phys. Lett. B **381**, 35 (1996).
  - [4] J. A. Hauger *et al.*, Phys. Rev. C **57**, 764 (1998).
  - [5] J. B. Elliott *et al.*, Phys. Lett. B **418**, 34 (1998).
  - [6] J. Lauret *et al.*, Phys. Rev. C **57**, R1051 (1998).
  - [7] B. K. Srivastava *et al.*, Phys. Rev. C **60**, 064606 (1999).
  - [8] J. A. Hauger *et al.*, Phys. Rev. C **62**, 024616 (2000).
  - [9] J. B. Elliott *et al.*, Phys. Rev. C **62**, 064603 (2000).
  - [10] R. P. Scharenberg *et al.*, Phys. Rev. C (to be published).
  - [11] J. P. Bondorf, A. S. Botvina, I. N. Mishustin, and K. Sneppen, Phys. Rep. **257**, 133 (1995).
  - [12] D. H. E. Gross, Rep. Prog. Phys. **53**, 605 (1990).
  - [13] D. H. E. Gross, Phys. Rep. **279**, 119 (1997).
  - [14] R. P. Scharenberg, Proceedings of the International Workshop XXVII on Gross Properties of Nuclei and Nuclear Excitations, Hirschegg, Austria, p. 237, GSI 1999.
  - [15] B. K. Srivastava, Proceedings of the International Workshop XXVII on Gross Properties of Nuclei and Nuclear Excitations, Hirschegg, Austria, p. 247, GSI 1999.
  - [16] X. Campi, J. Phys. A **19**, L917 (1986).
  - [17] X. Campi, Phys. Lett. B **208**, 351 (1988).
  - [18] X. Campi, Proceedings of the International School of Physics “Enrico Fermi,” Nuclear Collisions from the Mean-Field into the Fragmentation regime, CXII 331, (1991).
  - [19] W. Bauer *et al.*, Phys. Lett. **150B**, 53 (1985).
  - [20] W. Bauer *et al.*, Nucl. Phys. **A452**, 699 (1986).
  - [21] D. Stauffer and A. Aharony, *Introduction to Percolation Theory* (Taylor & Francis, London, 1992).
  - [22] W. Bauer, Phys. Rev. C **38**, 1297 (1988).
  - [23] P. Kreutz *et al.*, Nucl. Phys. **A556**, 672 (1993).
  - [24] M. Belkacem *et al.*, Phys. Rev. C **54**, 2435 (1996).
  - [25] P. F. Mastinu *et al.*, Phys. Rev. C **57**, 831 (1998).
  - [26] J. B. Elliott *et al.*, Phys. Rev. C **49**, 3185 (1994).
  - [27] S. Albergo, S. Costa, E. Costanzo, and A. Rubbino, Nuovo Cimento Soc. Ital. Fis., A **89**, 1 (1985).
  - [28] P. Bonche, S. Levit, and D. Vautherin, Nucl. Phys. **A436**, 265 (1985).
  - [29] S. Levit and P. Bonche, Nucl. Phys. **A437**, 426 (1985).
  - [30] H. R. Jaqaman, A. Z. Mekjian, and L. Zamick, Phys. Rev. C **29**, 2067 (1984).
  - [31] D. W. Heerman and D. Stauffer, Z. Phys. B: Condens. Matter **44**, 339 (1981).
  - [32] J. M. Carmona, J. Richert, and A. Tarancon, Nucl. Phys. **A643**, 115 (1998).
  - [33] J. M. Lattimer, C. J. Pethick, D. G. Ravenhall, and D. Q. Lamb, Nucl. Phys. **A432**, 646 (1985).